

Twin Roll Type 薄板連續鑄造에 대한 2次元응고문제의 數學的 Model

姜 忠吉*, 齊藤武雄**,

A Mathematical Model of Two-Dimensional Solidification
Problems for Twin Roll Type Strip Casting

C.G. Kang*, T.Saitoh**,

— 요 지 —

박판연속주조법은 용강으로부터 직접 제품을 제조하는 방법으로써 최근 에너지 절약, 신소재개발의 측면에서 주목되어지고 있다. 쌍로울식 연속주조법은 두개의 로울러 사이에 있어서 응고완료점의 제어가 극히 중요하다. 본 논문에서는 경제고정법에 의하여 액상역과 고상역을 동시에 해석하는 방법을 제안하여 이론해석의 결과를 실험결과와 비교한다.

또한 주조조건에 영향을 미치는 로울러 각속도, 로울러간의 간격이 응고형상에 미치는 영향을 밝히며 응고완료점이 로울러출구에 존재하는 주조조건을 구하여 주조가능 조건을 검토한다.

* 釜山大學校 工科大學 精密機械工學科

** 東北大學 工學部 機械工學第二學科

Nomenclature

$B(\phi)$: shape function of roll
 C : specific heat
 C_m^* : equivalent specific heat (see eq.(24))
 F : solidification front in solid zone
 G : solidification front in liquid zone
 h : vertical distance along the center line
 h_o : distance between the molten surface and the roll outlet
 H_o : roll spacing
 k : thermal conductivity
 L : latent heat of solidification
 Pe : Peclet number(= $U_o R_o / \alpha$)
 r, r' : radial coordinates
 R_o : roll radius
 t : time or Fourier number
 T : temperature
 T_o : initial temperature of molten metal
 T_f : solidus temperature (solidification temperature)
 T_l : liquidus temperature
 T_w : roll surface temperature
 U_o : casting speed
 U_r', U_ϕ' : velocities in the r and ϕ directions, respectively

Greek Symbols

α : thermal diffusivity
 β, β' : angles between radial directions and normal to solidification front
 $\delta(\phi)$: thickness of solidified layer
 η, ξ : independent variables (see eqs.(10) and (11))
 ρ : density
 σ_t : $=k_l / k_s$
 ϕ : angle
 ϕ_o : angle between the molten metal surface and the roll outlet

Subscripts and Superscripts

l : liquid region
 m : two-phase region
 s : solid region
 $*$: dimensionless quantity
 $'$: relevant to variables in the liquid region

1. Introduction

In recent years a growing interest has been concentrated on the twin-roll continuous casting(C.C.)processes which have many advantages over the existing other methods. The rapid solidification

process using twin-roll has been regarded to be promising from the following two view points: (i) Controlling the internal material structure such as the formation of quasi-steady stable phase, improvement or solubility limit, microcrystalline structure, prevention of segregation, and mechanical

properties, and (ii) effects of reduction of processes and energy saving, such as simplification of hot rolling process, manufacturing of difficult hot rolling materials and simplification of casting and rolling facilities.

Although the twin-roll C.C. process has good characteristics as mentioned above, its control seems somewhat to be difficult because of the existence of the deformation of the roll itself due to thermal expansion or thermal stresses owing to the narrow roll gap. Further, if solidification is completed before the minimum clearance point between rolls, then deformation of solid will occur. The plastic deformation of the material then has to be considered in this case.

For the abovementioned reasons, it is necessary to develop the efficient numerical tools to elucidate the complicated flow and heat transfer mechanism, which will be especially useful for designing the optimum twin-roll C.C. systems.

A thorough analysis for the two-dimensional solidification problems arising in the continuous casting in a moving slab including natural convection in the liquid phase was conducted by Kroeger and Ostrach[1]. They applied the conformal mapping technique and indicated that the recirculation flow is produced due to the strong natural convection in the liquid pool. However, they also pointed out that for the range of parameters investigated the natural convection had a negligible effect on the solid-liquid interface position. This suggestion is very interesting because the convection has only minor effect on determination of the solidification front despite the Grashof number is very large.

Solidification analyses for the C.C. of a slab have been done by Siegel[2,3,4], Koikkalainen et al.[5], Wang and Inoue[6], Lu and Zhi[7], Ohnaka[8], Ohnaka and Kobayashi[9], and so on.

While, the full solidification analysis for the twin-roll C.C. including flow and heat transfer in the liquid and solid regions is very scarce to the best of our knowledge. The only one is seemed to be the report of Miyazawa and Szelkely[10], in which the heat transfer, the flow of the solid and molten phases and the pressure distribution in the solid phase for the twin-roll rapid quenching of pure metallic materials were clarified by solving the onedimensional governing equations. They have indicated that there exists a narrow range of casting parameters, i.e. the roll spacing, the angular velocity of the rolls, the feed rate of the material, the physical properties of the material, that gives a stable mode of operation.

The C.C. problems including twin-roll technique have been reviewed by Szelkely(11), Ohnaka(12) and recently by Ohashi(13).

This paper presents a numerical methodology for the twodimensional heat transfer and flow phenomena in the liquid and solid regions in a twin-roll continuous casting system. The mathematical model presented covers the wide range of casting parameters since the two-dimensional transport in both phases was taken into account. Another objective is to provide a quantitative relationship between the principal casting parameters, such as the roll speed, the roll spacing, the initial temperature of molten material, the solidification profile with special attention

to the point of solidification.

2. Mathematical formulation

2.1 Numerical Model and the Governing Equations

Numerical model and the coordinate system are schematically shown in Fig.1. A molten metal is being fed from upstream into the nip of two the rolls rotating in opposite direction with an angular velocity ω . The surface of the molten metal O'P is always kept constant by overflowing the excess molten metal from the small leveling mouth. As soon as the molten materials is poured into the nip, solidification takes place on the roll surface which is cooled by recirculating water inside the roll.

Now, we define two coordinate systems: one is (r, ϕ) coordinate for the solid phase

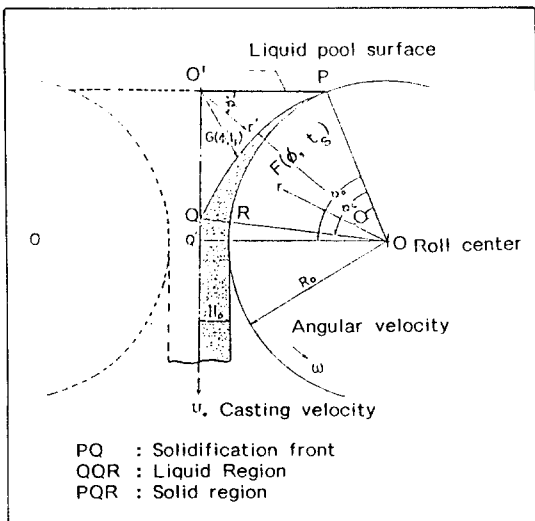


Fig. 1 Mathematical model and coordinate system for twin-roll continuous casting

with the origin at the center of the roll. Another one is (r, ϕ) coordinate for the solid phase with the origin at the center of the roll.

Another one is (r', ϕ') coordinate for the liquid phase with the origin at the point O'.

The solidified shell grew by the time $t=t$ is represented by the functions $F(\phi, t)$ and $G(\phi, t)$ in the solid and the liquid phase coordinates, respectively. If an appropriate casting condition is achieved, there exists a steady solidification profile which does not change with time.

The problem is then to find this steady solidification profile and the distributions of temperature and fluid velocities in both phases. A special attention is focused on the end point of solidification since the casting phenomena will change drastically depending whether this point would be located before the end point or not.

The following principal assumptions and restrictions may be made for the analysis in the development of the basic equations.

- 1) The slip between the roll and solidified shell in solid region is neglected.
- 2) The heat transfer is two-dimensional.
- 3) The relation between solidification rate and temperature in the solid-liquid coexisting region is linear.
- 4) Thermophysical properties are constant.
- 5) Mass flow rate in the normal direction to the center line is constant.

By virtue of the following dimensionless variables;

$$F^* = \frac{F}{R_0} \quad G^* = \frac{G}{R_0} \quad B^* = \frac{B}{R_0} \quad 2H_0^* = \frac{2H_0}{R_0} \quad T_0^* = \frac{T_0}{T_c - T_f}$$

$$\begin{aligned}
 T_i^* &= \frac{T_i}{T_o - T_f} & T_s^* &= \frac{T_s}{T_o - T_f} & T_f^* &= \frac{T_f}{T_o - T_f} \\
 r^* &= \frac{r}{R_o} & \phi^* &= \frac{\phi}{\phi_o} & r'^* &= \frac{r'}{R_o} & \phi'^* &= \frac{\phi'}{\phi_o'} \\
 \gamma'^* &= \frac{\beta'}{\phi_o'} & \gamma^* &= \frac{\beta}{\phi_o} & t_s^* &= \frac{\alpha_s t_s}{R_o} & t_i^* &= \frac{\alpha_i t_i}{R_o} \\
 \delta^*(\phi) &= \frac{\delta(\phi)}{R_o} & h_o^* &= \frac{h}{h_o}
 \end{aligned} \tag{1}$$

the governing equations for the above problems are described as below. Symbols* will be omitted hereafter for simplicity.

Solid region:

$$\frac{\partial T_s}{\partial t_s} = -\frac{P_{e,s}}{\phi_o} \frac{\partial T_s}{\partial \phi} \left[\frac{\partial^2 T_s}{\partial \gamma^2} + \frac{1}{\gamma} \frac{\partial T_s}{\partial \gamma} + \frac{1}{(\gamma \phi_o)^2} \frac{\partial^2 T_s}{\partial \phi^2} \right] \dots\dots\dots (2)$$

$$\gamma = B(\phi) \quad T = T_w \quad \dots\dots\dots (3)$$

$$\gamma = F(\phi, t_s) \quad T = T_f \quad \dots\dots\dots (4)$$

Liquid region:

$$\frac{\partial T_l}{\partial t_l} = -U(\phi) P_{e,l} \left[\sin \phi \frac{\partial T_l}{\partial \gamma'} + \frac{1}{\gamma' \phi_o'} \cos \phi \frac{\partial T_l}{\partial \phi'} \right] + \left[\frac{\partial^2 T_l}{\partial \gamma'^2} + \frac{1}{\gamma'} \frac{\partial T_l}{\partial \gamma'} + \frac{1}{(\gamma' \phi_o')^2} \frac{\partial^2 T_l}{\partial \phi'^2} \right] \dots\dots\dots (5)$$

$$\gamma' = G(\phi', t_l) \quad T_l = T_f \quad \dots\dots\dots (6)$$

$$\phi' = 1 \quad \frac{\partial T_l}{\partial \phi'} = 0 \quad \dots\dots\dots (7)$$

The heat balance equation at the solidification interface can be derived as shown Fig.2

Let β and β' be the angles between the coordinate axes and the normal direction to the solidification front, then the heat balance equation normal to the solidification front is give by the next equation.

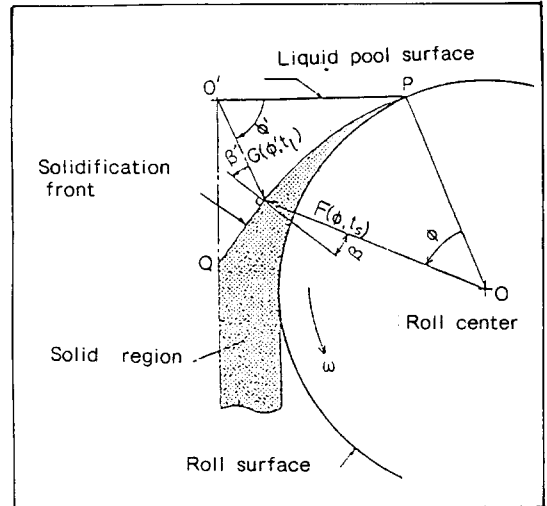


Fig. 2 Heat balance normal to solidification front.

$$\begin{aligned}
 \frac{\partial F}{\partial \phi} &= \frac{St_e}{P_{e,s}} \left(\frac{\phi_o}{R_o} \right) \left[\left\{ 1 + \left(\frac{R_o}{\phi_o} \frac{\partial F}{\partial \phi} \right)^2 \right\} \frac{\partial T_s}{\partial \gamma} \right. \\
 &\quad \left. - \sigma \frac{1}{\cos(\phi_o \gamma) \cos(\phi_o' \gamma')} \frac{\partial T_l}{\partial \gamma'} \right] \dots\dots\dots (8)
 \end{aligned}$$

Here, the nondimensional parameters including Stefan number and Peclet number have been defined as follows.

$$\begin{aligned}
 P_{e,s} &= \frac{U_o R_o}{\alpha_s} P & P_{e,l} &= \frac{U \phi' R_o}{\alpha_l} & \sigma &= \frac{K_l}{K_s} & \Phi &= \phi_o' \phi' \\
 \alpha_s &= \frac{k_s}{\rho C_s} & \alpha_l &= \frac{k_l}{\rho C_l} & St_\theta &= \frac{T_o - T_f}{L} C_s \dots\dots (9)
 \end{aligned}$$

2.2 Boundary Fixing Formulation

The problem to find the solidification front in twin-roll continuous casting belongs mathematically to the so-called moving(or free) boundary problem(MBP) which is characterized by having a moving interface dividing the relevant field into two regions. Such a problem becomes perfectly nonlinear because the positions of the moving fronts

are neither fixed in space nor known a priori. Various methods of solution for MBPs have been developed in this field and some of them can also be applied to the present C.C. problem.

One of the difficulties encountered in solving the multidimensional MBPs is handling the transient moving interface, which splits up between the liquid and solid domains. Here, the Boundary Fixing Method(BFM)[14,15]which was developed as one of the numerical methods for the MBP was adopted. The BFM considers arbitrary geometry of both the moving interface and the domain boundary via change of independent variable, thereby reducing the original problem into the one-dimensional fixed boundary problem encountered usually.

The next two independent variables are introduced for the present case.

Solid region:

$$\xi = \frac{\gamma - B(\phi)}{F(\phi, t_s) - B(\phi)} \quad \dots\dots\dots (10)$$

$$\eta = \frac{\gamma'}{G(\phi', t_i)} \quad \dots\dots\dots (11)$$

The correspondence between the physical plane and the transformed plane is schematically shown in Fig.3.

The resultant governing equations for solid region are written together with the boundary conditions as,

$$\begin{aligned} \frac{\partial T_s}{\partial t_s} = & -\frac{P_{e,s}}{\phi_o} \left(\frac{\partial T_s}{\partial \phi} + \frac{\partial T_s}{\partial \xi} \frac{\partial \xi}{\partial \phi} \right) + \left[\frac{1}{(F-1)^2} + \right. \\ & \left. + \frac{1}{R_s} \left(\frac{\partial \xi}{\partial \phi} \right)^2 \right] \frac{\partial^2 T_s}{\partial \xi^2} + \left[\frac{1}{\gamma F-1} + \frac{1}{R_s} \frac{\partial^2 \xi}{\partial \phi^2} \right. \end{aligned}$$

$$\left. - \frac{\partial \xi}{\partial t_s} \right] \frac{\partial T_s}{\partial \xi} + \frac{1}{R_s} \frac{\partial^2 T_s}{\partial \phi^2} + \frac{2}{R_s} \frac{\partial \xi}{\partial \phi} \frac{\partial^2 T_s}{\partial \xi \partial \phi} \quad \dots\dots\dots (12)$$

$$\xi=0 \quad T=T_w \quad \dots\dots\dots (13)$$

$$\xi=1 \quad T=T_f \quad \dots\dots\dots (14)$$

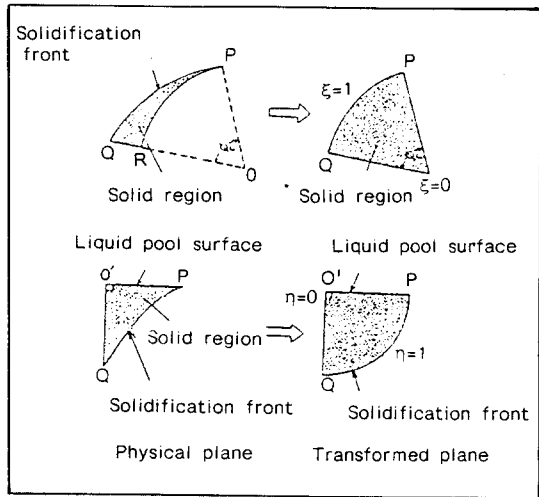


Fig. 3 Correspondence between physical plane and transformed plane

Further, the transformed equations for the liquid region are also written as,

$$\begin{aligned} \frac{\partial T_l}{\partial t_i} = & \left[\frac{1}{G(\phi', t_i)^2} + \frac{1}{R_l} \left(\frac{\partial \eta}{\partial \phi'} \right)^2 \right] \frac{\partial^2 T_l}{\partial \eta^2} \\ & + \left[\frac{1}{F'G(\phi', t_i)} + \frac{1}{R_l} \frac{\partial^2 \eta}{\partial \phi'^2} - \frac{U(\phi')P_{e,l}}{G(\phi', t_i)} \sin \phi \right. \\ & \left. - U(\phi')P_{e,l} \frac{1}{\sqrt{R_l}} \cos \phi \frac{\partial \eta}{\partial \phi'} - \frac{\partial \eta}{\partial t_i} \right] \frac{\partial T_l}{\partial \eta} \\ & - U(\phi)P_{e,l} \frac{1}{\sqrt{R_l}} \cos \phi \frac{\partial T_l}{\partial \phi'} + \frac{1}{R_l} \frac{\partial^2 T^2}{\partial \phi'^2} \\ & + \frac{2}{R_l} \frac{\partial \eta}{\partial \phi'} \frac{\partial^2 T_l}{\partial \eta \partial \phi'} \quad \dots\dots\dots (15) \end{aligned}$$

$$\eta=1, \quad T_l=T_f \quad \dots\dots\dots (16)$$

$$\phi'=1, \quad \frac{\partial T_l}{\partial \eta} = 0 \quad \dots\dots\dots (17)$$

Here, $\partial\xi/\partial\phi$, $\partial^2\xi/\partial\phi^2$, $\partial\eta/\partial\phi$, ... in the above equations are obtained by

$$\frac{\partial\xi}{\partial\phi} = -\xi \frac{1}{F-1} \frac{\partial F}{\partial\phi} \quad \dots\dots\dots (18)$$

$$\frac{\partial^2\xi}{\partial\phi^2} = -\frac{1}{F-1} [2 \frac{\partial F}{\partial\phi} \frac{\partial\xi}{\partial\phi} + \xi \frac{\partial^2 F}{\partial\phi^2}] \quad \dots\dots\dots (19)$$

$$\frac{\partial\eta}{\partial\phi} = -\eta \frac{1}{G(\phi', t_i)} \frac{\partial G}{\partial\phi'} \quad \dots\dots\dots (20)$$

$$\frac{\partial^2\eta}{\partial\phi'^2} = -\frac{1}{G(\phi', t_i)} [2 \frac{\partial G}{\partial\phi'} \frac{\partial\eta}{\partial\phi'} + \eta \frac{\partial^2 G}{\partial\phi'^2}] \quad \dots\dots\dots (21)$$

$$R_s = (r\phi_o)^2, \quad R_l = (r'\phi_o')^2 \quad \dots\dots\dots (22)$$

The heat balance equation at the solid-liquid interface is transformed to

$$\frac{\partial F}{\partial\phi} = \frac{St_e}{P_{e,s}} \left(\frac{\phi_o}{R_o}\right) \left[\frac{1}{F(\phi, t_s)-1} \left\{ 1 + \left(\frac{R_o}{\phi_o} \frac{\partial F}{\partial\phi}\right)^2 \right\} \frac{\partial T_s}{\partial\xi} - \frac{\sigma}{G(\phi', t_i)} \frac{1}{\cos(\phi_o\gamma) \cos(\phi_o'\gamma')} \frac{\partial T_l}{\partial\eta} \right] \quad \dots\dots\dots (23)$$

For the analysis in the liquid region, it is postulated that latent heat is rejected according to the solid fraction which is determined by liquid phase temperature. By use of previous assumption the equivalent specific heat in the coexisting region is expressed as,

$$C_m^* = C_l^* + \frac{L^*}{T_l^* - T_s^*} \quad \dots\dots\dots (24)$$

Here,

$$C_m^* = \frac{C_m}{C_s}, \quad C_l^* = \frac{C_l}{C_s},$$

$$L^* = \frac{L}{C_s(T_o - T_f)}, \quad T_l^* = \frac{T_l}{T_o - T_f} \quad \dots\dots\dots (25)$$

The computation of the energy equation(15) in the solid-liquid coexisting region was performed by using the specific heat shown by the above equation.

However, the usual equations were solved other than this region.

2.3 Numerical Procedure

The solution of the steady continuous casting problem in twin-roll geometry was obtained as a steady ultimate solution of a false transient problem. First, the solidification profile and the initial temperature distributions in both liquid and solid phases were assumed for given casting conditions. Then, the temperature distributions in both phases are obtained by use of equations(12) and (15) with boundary conditions(13), (14), (16), and (17). Next, the new solidification front $F(\phi, t)$ is calculated by virtue of equation(23) by using newly obtained temperature information in the vicinity of the interface. This procedure is repeated until the final steady solidification front is attained.

The usual 3-point explicit finite difference scheme was used for the computation of energy equations. Simplified block flow chart of computations appears in fig.4

The computer running time for a typical case was approximately 10 seconds on SX-1 of Tohoku University. The principal data used for computation were listed in Table 1. The materials selected are Sn-15Pb and steel.

Table 1. Physical Constants and properties used in calculations

thermal conductivity in solid zone	k_s	50.2(W/mk)
thermal conductivity in liquid zone	k_l	21.0(W/mk)
specific heat in liquid zone	C_l	0.23(KJ/Kg K)
density in solid zone	ρ	7200(Kg/m ³)
solid line temperature	T_s	208(°C)
liquid line temperature	T_l	183(°C)

3. Numerical Results and Discussion

In this section, the numerical results for typical casting conditions will be shown and the comparison with those of the experimental data and one-dimensional theory will be made.

The results of computation including heat transfer in both phases and fluid flow in the liquid phase is indicated in Fig.5(a) in the case of $2H_o^*=0.073$, $Pe_{s,l}=47.2$, $\sigma=0.417$ and $T_p^*=7.1$. The isotherms are shown by the solid lines including the solidus line. The experimental solidus and liquidus lines are also shown by the broken lines. The experiment [16] was done separately with this study and detailed description is omitted. However, it is noted here that the temperature measurement was performed by placing a thin plate in which thermocouples were embedded just beneath the surface and the data acquisition was made by using a high-speed data logger. The comparison of the present calculation results and the experimental data reveals a moderate coincidence. In Fig.4, the computed result without consideration of heat transfer and fluid flow in the liquid

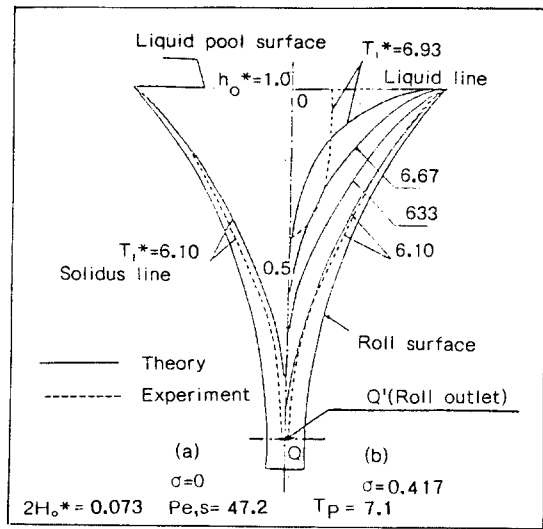


Fig.5 Solidified shell profile and isotherms in the liquid region

phase is depicted for the purpose of comparison. It is seen that consideration of full heat and fluid flow bring forth a closer result to the experimental data. However, its difference is not so large. This consequence is in line with that of Kroeger and Ostrach [1] who analyzed a plane continuous casting problem via a conformal mapping method and showed that the natural convection effect has a negligible effect on the solid-liquid interface position as far as in the range of the parameters investigated by them.

Figure 6 plots the temperature distribution in the vertical center plane ($0'Q'$ plane) of the liquid domain under the same conditions as in Fig.5(a). The squares and the solid line designate experimental data and theoretical result, respectively. The entire coincidence is fairly good except the solid-liquid coexisting region ($T_1^*=6.1-6.9$) where a slight difference is seen.

The difference of the experimental and theoretical results in the end point

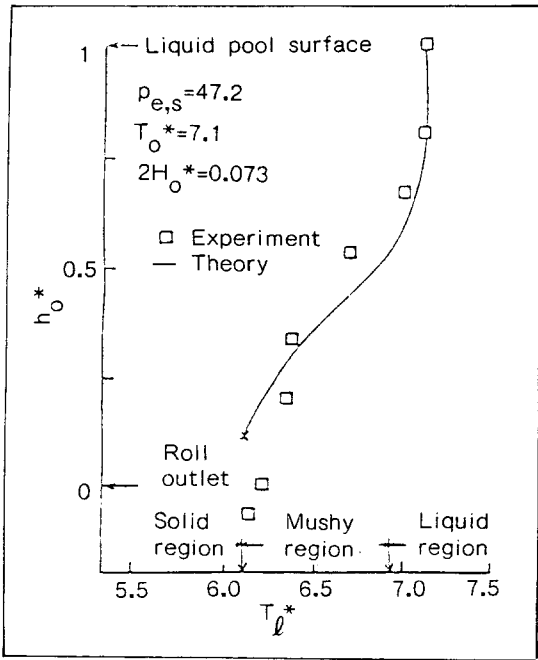


Fig. 6 Temperature distribution along the center line of molten material. The calculated result (solid line) is compared with the experimental results (open square)

solidification could be considered as roll surface temperature variation, heat generation by deformation in the solid region.

Figure 7 shows the solidified shell thickness versus angle measured from the initiation point P (see Fig. 1). The figure compares the experimental results with the theoretical ones obtained under assumptions of, (i) one-dimensional heat flow, (ii) two-dimensional heat flow without consideration of liquid side heat transfer and fluid flow, and (iii) full solution considering all of these. It is seen from the figure that the full solution gives the most accurate result since the experimental data can be considered to be reliable at present (no other comparable data are available).

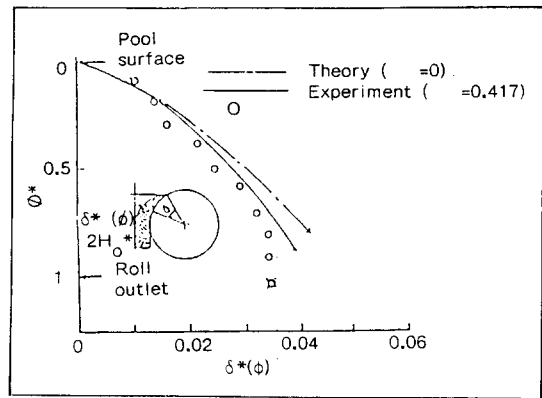


Fig. 7 Comparison between calculated and experimental values for solidification shell thickness. Calculation according to one dimensional theory is also shown in the figure by a broken line

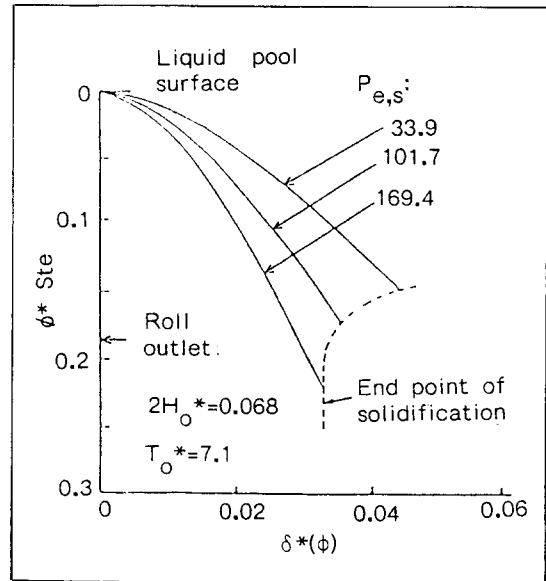


Fig. 8 Variation of solidification shell thickness with the roll spacing

It is noted here that one-dimensional analysis does not provide a good result. This point is especially important since most of past studies have based on this assumption [10]. The heat and the fluid flow in the vicinity of end of solidification

point(point Q) becomes two-dimensional since the solidified layer gets thick in this region.

Although it is deduced that convection has minor effect on determination of the solidification front, the analysis of convection pattern in the liquid region will be very important from the view point of eliminating segregation and controlling the grain size of the wasted materials.

The effect of rotation speed of roll on solidification is shown in Fig.8 for roll spacing $2H_o^*=0.068$ and initial temperature $T_o^*=7.1$. The ordinate designates dimensionless angle and abscissa the solidified layer thickness. The rotation speed of roll is included in the Peclet number, Pe_s . The value of Pe_s when end point of solidification just coincides with the minimum gap position Q'(i.e.roll outlet, shown by an arrow in the figure)is around 102. The complete solidification point

moves downward of the minimum gap point if the Pe_s exceeds this critical value. Whether end point of solidification is located before the minimum gap point or not may be an important criterion since deformation of the solid, i.e. plastic flow of the solid, will occur if solidification is completed before the material reaches the minimum clearance position. This point will also important from the view point of quality control of the cast materials, for example, prevention of crack in the center portion of the cast material, which has been clarified by the experiment[17].

Figure 9 indicates the effect of variation of the roll spacing on the solidification shell thickness in case of $T_o^*=7.1$ and $Pe_s=67.7$. It is seen that increase of the roll spacing has only a slight influence upon the solidification profile. Further, end point of

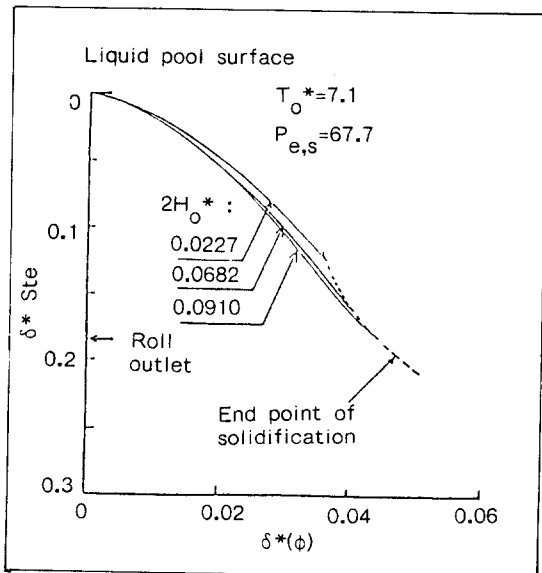


Fig. 9 Variation of solidified shell thickness with the roll spacing

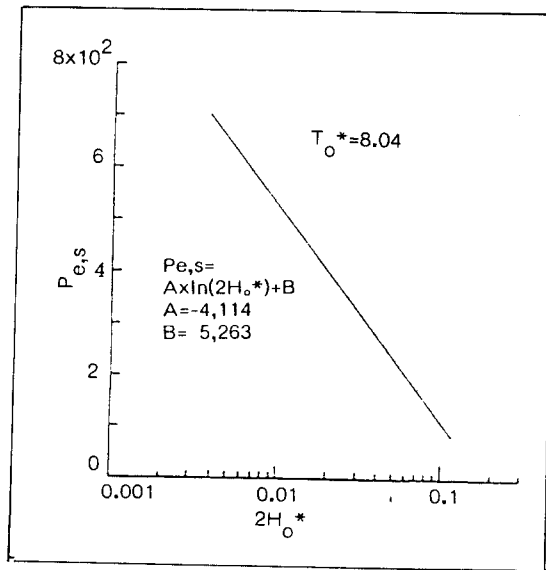


Fig. 10 Showing the relationship between the Peclet number and the roll spacing when end point of solidification just coincides with the minimum clearance point

solidification moves downward with increase of the roll spacing.

Figure 10 shows a relationship between the pecllet number, Pe_s and the roll spacing $2H_0^*$ when end point of solidification just coincides with the minimum clearance point Q' under a condition of $T_0^*=8.04$ and $\dots=0.417$. As mentioned earlier, this diagan may be helpful in designing the real twin-roll casting machine.

The relation can be expressed by the following simple equation:

$$Pe_s = -4.11 \ln(2H_0^*) + 5.26 \quad (26)$$

4. Concluding Remarks

A numerical algorithm for the two-dimensional solidification problem in the twin-roll continuous casting system has been presented in this paper. Attention was focused on the elucidation of flow and heat transfer characteristics in both liquid and solid phases. The present mathematical model can be applied to general full Navier-Stokes and energy equations, thereby covering the wide range of casting conditions. The boundary fixing method is adopted to handle the moving boundary and the resultant transformed governing equations for the solid and liquid regions were solved separately by using usual explicit-type finite difference scheme. The following conclusions may be drawn from the present study.

(i) A general numerical methodoogy was presented and the quantitative relationship between the important control parameters in continuous casting of twin-roll type, such

as the roll speed, the roll gap, the initial temperature of molten materials, the material properties, the solidification profile, and the end point of solidification and the like was clarified in detail. The present numerical results were compared with experimental results obtained separately to check the validity of the proposed method.

(ii) The influence of liquid phase heat transfer on the entire solidification profile is not significatn, which is in accordance with the consequence presented by Kroeger and Ostrach [1]. This implies that a simplified analysis which neglects the heat transfer in the liquid phase would yield a moderate result as far as the solidification front is concerned.

(iii) Whereas the speed of roll has a great influence on the solidification profile, the influence of the roll spacing is minor.

In closing, it is noted here that a thorough two-dimensional analysis including full heat and flow equations will be necessary to get more insight into natural convection effect in the liquid phase. Such task will be important in reducing segregation and also in improving material quality.

Reference

1. P.G.Kroeger and S.Ostrach: The Solution of a Two-Dimensional Freezing Problem Including Convection Effects in the Liquid Region, Int. J. Heat Mass Transfer. 17-10(1974) p.1191.
2. R.Siegel: Analysis of Solidification Interface Shape during Continuous Casting of a Slab: Int. J. Heat Mass Transfer, 21-11(1978) p.1421.

3. R.Siegel: Solidification Interface Shape for Continuous Casting in an Offset Mold-Two Analysis Methods, J.Heat Transfer, Trans. ASME, 106(1984), p237.
4. R.Siegel: Two-Region Analysis of Interface Shape in Continu Continuous Casting with Superheated Liquid, J. Heat Transfer, Trans. ASME, 106(1984), p506.
5. P.Koikkalainen, E.Laitnen, S. Louhenkilpi, Neittaanmaki and L. Holappa: FE-Modelling of Continuous Casting Problem, Proc. Int. Conf. on Comp. Mech., Vol.III(1986)p29.
6. Z.G Wang and T.Inoue, Analysis of Temperature and Elastic-Viscoplastic Stress during Continuous Process, proc. Int. Conf. on Comp. Mech. Vol II(1986) p103.
7. Z.F. Lu and J.Zhi: Mathematical Modelling of Three-Dimensional Flow Field in the Mold Region in Continuous Casting System, Proc. Int. Conf. on Comp. Mech., Vol.II(1986)p23.
8. I.Ohnaka: Modelling of Solidification Structure of Casting, Proc. MRS-Europe symp., Strasbourg(1986)p1.
9. I.Ohnaka and K.Kobayashi: Flow Alysis during Solidification the Direct Finite Difference Method, Trans. of the Iron and teel Inst. of Japan, vol.26, p781.
10. K.Miyazawa and J.Szelkely: A Matnematical Model of the slat Cooling Process Using the Twin Roll Technique. Stall Trans., 12A-6(1981), p. 1047.
11. J.Szekely: In Free Boundary Problems: Theory and Plications, vol.II(1981), p. 283.
12. I.Ohnaka: Production of Amorphous Alloy Materials and Rapid tenching Techniques, J.JSME, 88-802(1985), p. 1060.
13. T.Ohashi: Present Status of Continuous Casting of Steel and Nature D e v e l o p m e n t s , Nipponkinzokugakkaihou, 25(1986), p. 505.
14. T. Saitoh: Numerical Method for Multi-Dimentional Freezing Problems in Arbitrary Domains, Trans, ASME, J. Heat Transfer, 100-2(1978)p.294.
15. T.Saitoh: Introduction Numerical Heat Transfer, Yokendo Pulb.Co., Ltd.(1986)
16. H.Hojo, C.G. Kang, K.Kato, N. Tamagawa, and H.Yaguchi: The Study on Casting Condition and Solidification Characteristics of Twin-Roll Type in Strip Casting Proc. 37th Japanese Joint Conf. Tech. Plasticity(1986)p.517.